Statistical properties of the localization measure of chaotic eigenstates and the spectral statistics in a mixed-type billiard

Benjamin Batistić⬤, Črt Lozej, and Marko Robnik⬤

CAMTP-Center for Applied Mathematics and Theoretical Physics, University of Maribor, Mladinska 3,
SI-2000 Maribor, Slovenia, European Union

We study the quantum localization in the chaotic eigenstates of a billiard with mixed-type phase space [J. Phys. A: Math. Gen. **16**, 3971 (1983); **17**, 1049 (1984)], after separating the regular and chaotic eigenstates, in the regime of slightly distorted circle billiard where the classical transport time in the momentum space is still large enough, although the diffusion is not normal. This is a continuation of our recent papers [Phys. Rev. E **88**, 052913 (2013); **98**, 022220 (2018)]. In quantum systems with discrete energy spectrum the Heisenberg time $t_H = 2\pi\hbar/\Delta E$, where ΔE is the mean level spacing (inverse energy level density), is an important timescale. The classical transport timescale t_T (transport time) in relation to the Heisenberg timescale t_H (their ratio is the parameter $\alpha = t_H/t_T$) determines the degree of localization of the chaotic eigenstates, whose measure A is based on the information entropy. We show that A is linearly related to normalized inverse participation ratio. The localization of chaotic eigenstates is reflected also in the fractional power-law repulsion between the nearest energy levels in the sense that the probability density (level spacing distribution) to find successive levels on a distance S goes like $\propto S^\beta$ for small S, where $0 \leqslant \beta \leqslant 1$, and $\beta = 1$ corresponds to completely extended states. We show that the level repulsion exponent β is empirically a rational function of α, and the mean $\langle A \rangle$ (averaged over more than 1000 eigenstates) as a function of α is also well approximated by a rational function. In both cases there is some scattering of the empirical data around the mean curve, which is due to the fact that A actually has a distribution, typically with quite complex structure, but in the limit $\alpha \to \infty$ well described by the beta distribution. The scattering is significantly stronger than (but similar as) in the stadium billiard [Nonlin. Phenom. Complex Syst. (Minsk) **21**, 225 (2018)] and the kicked rotator [Phys. Rev. E **91**, 042904 (2015)]. Like in other systems, β goes from 0 to 1 when α goes from 0 to ∞. β is a function of $\langle A \rangle$, similar to the quantum kicked rotator and the stadium billiard.

I. INTRODUCTION

Quantum chaos (or more generally, wave chaos) deals with phenomena in the quantum domain, which are signatures of the classical chaos in the corresponding classical systems [1–3]. The classical dynamics as the ray dynamics of the quantum wave functions is, for example, an analogy of the relationship between the Gaussian ray optics and the wave phenomena of the Maxwell equations describing the electromagnetic field. The classical and the quantum descriptions are connected theoretically through the semiclassical mechanics, which is the short wavelength approximation of the underlying wave field. We also might say that classical dynamics is the short wavelength limit, but only up to a certain scale determined by the Planck constant $\hbar$, of the quantum dynamics. The fundamental difficulty is that the two limits $\hbar \to 0$ (the classical limit) and $t \to \infty$ (asymptotic time limit) do not commute.

In the classically integrable Hamiltonian systems with f degrees of freedom the semiclassical theory predicts that the quantum eigenstates (in the $2f$-dim phase space, represented by Wigner functions [4] or Husimi functions [5]) are associated with the classical f-dim invariant tori. In the case of classical ergodic systems, the eigenstates are microcanonical

[uniformly spread over the $(2f - 1)$-dim energy surface]. In the case of the mixed-type classical phase space, where regular regions covered by the invariant tori coexist with the chaotic sea (one or more chaotic invariant regions), we have the generic structure (almost all systems are of this type), where we have to distinguish between the quantum regular and irregular (chaotic) eigenstates, an idea proposed qualitatively already in 1973 by Percival [6]. This line of thought lead to the Principle of Uniform Semiclassical Condensation of Wigner functions [7], based on work of Berry [8], Shnirelman [9], Voros [10], and further developed by Veble, Robnik and Liu [11]. The Wigner functions of the eigenstates condense uniformly on the classical invariant component in the classical phase space, and this principle (PUSC) has a great predictive power as demonstrated, e.g., in Ref. [11].

The classical dynamics of bounded Hamiltonian systems determines also the statistical properties of the discrete energy spectra of the corresponding eigenstates. For the classically regular motion it predicts Poissonian energy level statistics, while in the classically fully chaotic (ergodic) systems the statistics of random matrix theory (RMT) applies, as conjectured by Bohigas, Giannoni, and Schmit [12] in 1984, also by Casati, Valz-Gris, and Guarneri [13], proven by Berry [14], Sieber and Richter [15], and by Haake and coworkers [16–19],

using the semiclassical techniques based on the Gutzwiller's periodic orbit theory (see Refs. [20–24] and also the books by Stöckmann [1] and Haake [2]).

The intermediate case of the mixed-type Hamilton systems was treated first theoretically by Berry and Robnik [25] and has been analyzed later on in many studies, most accurately by Prosen and Robnik [26]. In this picture the parameter ρ_1 plays the crucial role, being the relative fraction of the phase space volume occupied by the regular regions in the classical phase space, and it also is the relative density of the regular energy levels in the total quantum spectrum of the underlying system. The spectral statistics for the regular levels is Poissonian.

If there are chaotic regions with the relative volume fractions (and corresponding energy level densities) $\rho_2, \rho_3, \ldots$, then for each of them the RMT statistics applies. Usually, the dominant chaotic region is by far the largest one, $\rho_2 \gg \rho_3, \ldots$, so that the smaller chaotic regions can be neglected, and we have $\rho_1 + \rho_2 = 1$.

The best mathematical description of such a mixed-type case is in terms of the gap probability $E(S)$. This is the probability that an energy interval (after unfolding, i.e., reducing the mean energy level density to unity) is empty of levels. Clearly, if regular and chaotic eigenstates are not correlated, being statistically independent of each other, then the gap probabiliy simply factorizes, that is

$$E(S) = E_P(\rho_1 S)\, E_{\mathrm{RMT}}(\rho_2 S), \tag{1}$$

where P and RMT refer to the Poissonian and RMT statistics, respectively. The Poissonian is $E_P(S) = \exp(-S)$. For the GOE level spacing distribution, which applies if the time reversal symmetry (or any other antiunitary symmetry) exists, the well-known Wigner distribution (Wigner surmise) is an excellent analytical approximation,

$$P_W(S) = \frac{\pi S}{2} \exp\left(-\frac{\pi S^2}{4}\right), \tag{2}$$

while the corresponding gap probability is

$$E_W(S) = 1 - \mathrm{erf}\left(\frac{\sqrt{\pi}S}{2}\right) = \mathrm{erfc}\left(\frac{\sqrt{\pi}S}{2}\right). \tag{3}$$

The level spacing distribution $P(S)$ is the second derivative of the gap probability $P(S) = d^2 E(S)/dS^2$, and therefore in this case given by

$$P_{BR}(S) = e^{-\rho_1 S} e^{-\frac{\pi \rho_2^2 S^2}{4}} \left(2\rho_1 \mu_2 + \frac{\pi \rho_2^3 S}{2}\right) \tag{4}$$

$$+ e^{-\rho_1 S} \rho_1^2 \mathrm{erfc}\left(\frac{\sqrt{\pi}\rho_2 S}{2}\right),$$

as derived by Berry and Robnik [25]. Of course, $\rho_2 = 1 - \rho_1$. The gap probability $E(L)$ is just a special case of $E(k, L)$ probability of finding k levels on an interval of length L, namely, $E(L) = E(0, L)$. For more details about the $E(k, L)$ probabilities with $k > 0$, see Ref. [26].

The above statements are correct only if the chaotic states are uniformly extended over the classical invariant chaotic component. This condition, however, is not always satisfied. The phenomenon of dynamical (or quantum) localization can occur, first discovered and further explored by Chirikov, Izrailev, and Shepelyansky [27] in the quantum kicked rotator

(QKR) introduced by Casati, Chirikov, Izrailev, and Ford [28] as a model system, and later extensively studied in particular by Izrailev [29–33]. The QKR is a time periodic (Floquet) system. The time independent chaotic systems are exemplified by the 2-dim billiard systems. Borgonovi, Casati, and Li [34] have studied from this point of view the stadium billiard of Bunimovich [35]. See also the review by Prosen [36]. The case of mixed-type billiard has been studied recently by Batistić and Robnik [37–39].

The criterion for localization is in terms of the ratio

$$\alpha = \frac{t_H}{t_T} \tag{5}$$

of the Heisenberg time t_H and the classical transport time t_T. Here, $t_H = 2\pi\hbar/\Delta E$, with ΔE being the mean energy level spacing (inverse energy level density), which is an important timescale in any quantum system with discrete energy spectrum, while t_T is the purely classical ($\hbar$-independent) diffusion time, or typical time needed for an ensemble of initial sharply distributed momenta to spread uniformly over the classical chaotic component. If $\alpha \ll 1$, then the chaotic eigenstates are maximally localized, while if $\alpha \gg 1$, then the eigenstates are maximally extended, but in between we have the partially localized eigenstates. The degree of localization can be measured most easily in terms of the Husimi function [5], which is positive definite and can be treated as quasiprobability density. There are three main localization measures: A, the information entropy measure, C the correlation localization measure, and nIPR the normalized inverse participation ratio. As recently shown [38,40], they are all proportional to each other (linearly related) and thus equivalent. The energy spectra of the localized chaotic eigenstates can be well described by the fractional power law level repulsion, $P(S) \propto S^\beta$, for small S, and $\beta \in [0, 1]$: $\beta = 0$ corresponds to the maximal localization and Poissonian statistics, while $\beta = 1$ corresponds to the maximal extendedness (delocalization) and the RMT statistics. It has been found that β is a function of A, they are linearly related in QKR and in the stadium billiard, as well as in the present work. It is also an almost rational function of α.

The local behavior of $P(S)$ at small S can be globalized by approximating it by the well known Brody distribution [41,42], described by the following formula

$$P_B(S) = cS^\beta \exp(-dS^{\beta+1}), \tag{6}$$

where by normalization of the total probability and the first moment we have

$$c = (\beta + 1)d, \quad d = \left[\Gamma\left(\frac{\beta+2}{\beta+1}\right)\right]^{\beta+1}, \tag{7}$$

with $\Gamma(x)$ being the gamma function. It interpolates the exponential and Wigner distribution as β goes from 0 to 1. The corresponding gap probability is

$$E_B(S) = \frac{1}{\gamma(\beta+1)} Q\left[\frac{1}{\beta+1}, (\gamma S)^{\beta+1}\right], \tag{8}$$

where $\gamma = \Gamma(\frac{\beta+2}{\beta+1})$ and $Q(a, x)$ is the incomplete gamma function

$$Q(a, x) = \int_x^\infty t^{a-1} e^{-t} dt. \tag{9}$$

Here the only parameter is β, the level repulsion exponent in Eq. (6), which measures the degree of localization of the chaotic eigenstates. By replacing $E_{\mathrm{RMT}}(S)$ with $E_B(S)$ we get the so-called Berry-Robnik-Brody (BRB) distribution, which generalizes the Berry-Robnik (BR) distribution such that the localization effects are included [37]. In this way the problem of describing the energy level statistics is empirically solved. However, the theoretical derivation of the Brody distribution for the localized chaotic states remains an important open problem. One important theoretical plausibility argument by Izrailev in support of Brody (or Brody-like) intermediate level spacing distribution is that the joint level distribution of Dyson circular ensembles can be extended to noninteger values of the exponent β [33]. Our recent numerical results show that Brody distribution is good in describing real data [37,38,43,44].

This paper is a continuation of our recent works on the mixed-type billiard [45–47], classical and quantal. The role of the divided phase space and of the localization effects of chaotic eigenstates has been extensively studied in Refs. [37–39].

In the very recent papers on the classical dynamics in the stadium billiard [48] we have carefully investigated the classical diffusion and transport properties, while in Refs. [40,49] we have performed a complete analysis of the following quantal aspects: we have shown that nIPR and A are equivalent, A has a distribution on a compact interval $[0, A_0]$, very well described by the beta distribution. It turns out in our analysis that A_0 is approximately equal to 0.7 for maximally extended Poincaré-Husimi functions, like in the present work, although we do not have a theory for it. We have shown some representative Poincaré-Husimi functions of various degrees of localization A. The mean value $\langle A \rangle$ is approximately a rational function of α, the standard deviation σ of A is analyzed, and we have shown that the level repulsion exponent β is a linear function of $\langle A \rangle$, and an almost rational function of α, consistently with the other properties. Finally, σ seems to be a unique function of β.

The purpose of the present paper is to carry out the same complete analysis of the chaotic eigenstates in the mixed-type billiard introduced in Refs. [45,46], showing that all statistical properties of localized chaotic eigenstates are universal, if the system's chaotic component is without pronounced stickiness regions: The distribution $P(A)$ is beta distribution. However, if the stickiness regions exist and are pronounced, then $P(A)$ is nonuniversal, it can have several maxima (usually two), and each secondary maximum can be attributed to a stickiness region.

We should emphasize the fact that 2-dim billiards are quite typical Hamilton systems, as they can display all the general phenomena found in other smooth Hamilton systems, but are as model systems much easier to study, theoretically and numerically, classically and quantally. Therefore, we certainly may expect that our results are quite typical for general Hamilton systems. These include, e.g., hydrogen atom in strong magnetic field, Dicke model, quantum dots, molecules, nuclea, mesoscopic systems, microwave resonators, optical microcavity lasers, etc. See the discussion in Sec. VI.

The paper is organized as follows. In Sec. II we define the billiard system, the Poincaré-Husimi functions, introduce a method to separate regular and chaotic eigenstates, and define the localization measures A and nIPR, and we show that they are equivalent. In Sec. III we show the dependence of the moments of A on α and present some typical Poincaré-Husimi functions. In Sec. IV we calculate the localization measures A and their distribution functions in various classical dynamical regimes. In Sec. V we analyze the energy spectra and their statistical properties (the level spacing distributions) as functions of α in various classical dynamical regimes. In Sec. VI we draw the conclusions and discuss them in the context of further open problems.

II. THE BILLIARD SYSTEM, DEFINITION OF THE POINCARÉ-HUSIMI FUNCTIONS, SEPARATION OF REGULAR AND CHAOTIC EIGENSTATES, AND THE LOCALIZATION MEASURES A AND NIPR

A. The billiard system

The mixed-type billiard system $\mathcal{B}$ in this paper has been introduced in Refs. [45,46] and has been further studied by many others as a model system, most extensively recently by Lozej and Robnik [47]. Its shape is defined by the complex quadratic conformal map from the unit circle $|z| = 1$ in the z plane onto the physical w plane,

$$w = z + \lambda z^2, \qquad (10)$$

where the family parameter λ goes from 0 to $1/2$: At $\lambda = 0$ we have the integrable circular billiard, for $0 < \lambda < 1/4$ it is a convex shape having mixed-type phase space, in particular, we have the Lazutkin's caustics in the w plane and corresponding invariant curves in the phase space. For $\lambda = 1/4$ it is still convex but has a zero curvature point at $z = -1$ and therefore (Mather's theorem) all Lazutkin's tori are destroyed, allowing for ergodicity, which, however, does not yet occur, as we numerically still find islands of stability. For $1/4 < \lambda < 1/2$ it is nonconvex but still has a smooth boundary and very tiny islands of stability (regular islands), while for $\lambda = 1/2$ it has a cusp singularity at $z = -1$ and has been proven by Markarian [50] to be ergodic. Thus, the system is an interesting and quite well explored one-parameter family of billiards going from the integrable circle billiard to a rigorously ergodic and fully chaotic billiard, having mixed-type dynamics for the intermediate values of λ. A recent very extensive survey of the chaotic phase space has been performed by Lozej [51].

For a 2D billiard the most natural coordinates in the phase space (s, p) are the arclength s round the billiard boundary in the mathematically positive sense (counterclockwise). $s \in [0, \mathcal{L}]$, where $\mathcal{L}$ is the circumference, in our case starting at $s = 0$ at the point $z = 1$. The sine of the reflection angle θ, which is the component of the unit velocity vector tangent to the boundary at the collision point, equal to $p = \sin \theta$, is the canonically conjugate momentum to s. These are the Poincaré-Birkhoff coordinates. The bounce map $(s_1, p_1) \rightarrow (s_2, p_2)$ is area preserving [52], and the phase portrait does not depend on the speed (or energy) of the particle.

Quantum mechanically we have to solve the stationary Schrödinger equation, which in a billiard is just the Helmholtz equation,

$$\Delta \psi + k^2 \psi = 0, \qquad (11)$$

with the Dirichlet boundary conditions $\psi|_{\partial\mathcal{B}} = 0$. The energy is $E = k^2$. The important quantity is the boundary function,

$$u(s) = \mathbf{n} \cdot \nabla_{\mathbf{r}}\psi(\mathbf{r}(s)), \tag{12}$$

which is the normal derivative of the wave function ψ at the point s ($\mathbf{n}$ is the unit outward normal vector). It satisfies the integral equation

$$u(s) = -2 \oint dt \, u(t) \, \mathbf{n} \cdot \nabla_{\mathbf{r}} G(\mathbf{r}, \mathbf{r}(t)), \tag{13}$$

where $G(\mathbf{r}, \mathbf{r}') = -\frac{i}{4}H_0^{(1)}(k|\mathbf{r} - \mathbf{r}'|)$ is the Green function in terms of the Hankel function $H_0^{(1)}(x)$. It is important to realize that the boundary function $u(s)$ contains complete information about the wave function at any point $\mathbf{r}$ inside the billiard by the equation

$$\psi_m(\mathbf{r}) = - \oint dt \, u_m(t) \, G(\mathbf{r}, \mathbf{r}(t)). \tag{14}$$

Here m is just the index (sequential quantum number) of the mth eigenstate.

B. The Poincaré-Husimi functions

Now we go over to the quantum phase space. We can calculate the Wigner functions [4] based on $\psi_m(\mathbf{r})$. However, in billiards it is advantageous to calculate the Poincaré-Husimi functions. The Husimi functions [5] are generally just Gaussian smoothed Wigner functions. Such smoothing makes them positive definite, so that we can treat them somehow as quasiprobability densities in the quantum phase space, and at the same time we eliminate the small oscillations of the Wigner functions around the zero level, which do not carry any significant physical contents, but just obscure the picture. Thus, following Tualle and Voros [53] and Bäcker *et al.* [54], we introduce [38,39] the properly $\mathcal{L}$-periodized coherent states centered at (q, p) as follows:

$$c_{(q,p),k}(s) = \sum_{m\in\mathbf{Z}} \exp\{i\,k\,p\,(s - q + m\mathcal{L})\} \tag{15}$$

$$\times \exp\left[-\frac{k}{2}(s - q + m\mathcal{L})^2\right].$$

The Poincaré-Husimi function is then defined as the absolute square of the projection of the boundary function $u(s)$ onto the coherent state, namely,

$$H_m(q, p) = \left| \int_{\partial\mathcal{B}} c_{(q,p),k_m}(s) \, u_m(s) \, ds \right|^2. \tag{16}$$

C. The localization measures A and nIPR

The *entropy localization measure* of a *single eigenstate* $H_m(q, p)$, denoted by A_m is defined as

$$A_m = \frac{\exp I_m}{N_c}, \tag{17}$$

where

$$I_m = -\int dq \, dp \, H_m(q, p) \ln[(2\pi\hbar)^f H_m(q, p)] \tag{18}$$

is the information entropy. Here f is the number of degrees of freedom (for 2D billiards $f = 2$, and for surface of section
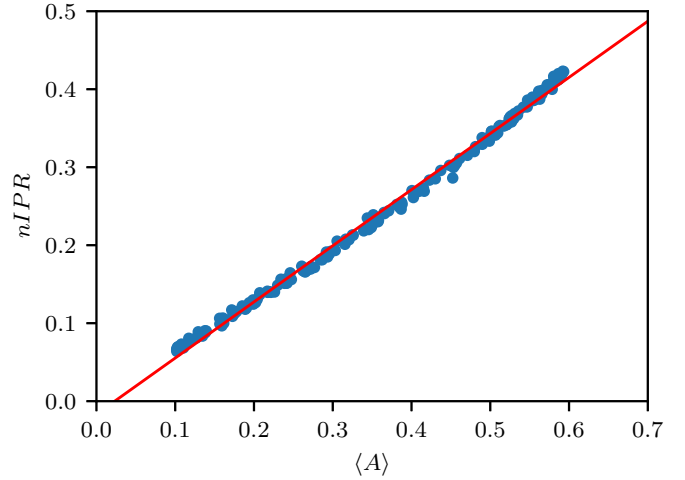

FIG. 1. The normalized inverse participation ratio as a localization measure, as a function of A. They are linearly related and thus equivalent. We have used the chaotic states with $M \geqslant M_t = 0.5$. The slope is 0.72 and the intercept -0.017.

it is $f = 1$) and N_c is a number of cells on the classical chaotic domain, $N_c = \Omega_c/(2\pi\hbar)^f$, where Ω_c is the classical phase space volume of the classical chaotic component. In the case of the uniform distribution (extended eigenstates) $H = 1/\Omega_C = $ const. the localization measure is $A = 1$, while in the case of the strongest localization $I = 0$, and $A = 1/N_C \approx 0$. The Poincaré-Husimi function $H(q, p)$ Eq. (16) (normalized) was calculated on the grid points (i, j) in the phase space (s, p), and we express the localization measure in terms of the discretized function. In our numerical calculations we have put $2\pi\hbar = 1$, and thus we have $H_{ij} = 1/N$, where N is the number of grid points, in case of complete extendedness, while for maximal localization we have $H_{ij} = 1$ at just one point, and zero elsewhere. In all calculations have used the grid of 400×400 points, thus $N = 160\,000$.

As mentioned in the Introduction, the definition of localization measures can be diverse, and the question arises to what extent are the results objective and possibly independent of the definition. Indeed, in Ref. [38], it has been shown that A and C (based on the correlations) are linearly related and thus equivalent. Moreover, we have introduced [40] also the normalized inverse participation ratio $R = $ nIPR, defined as follows:

$$R = \frac{1}{N} \frac{1}{\sum_{i,j} H_{ij}^2}, \tag{19}$$

for each individual eigenstate m. However, because we expect fluctuations of the localization measures even in the quantum ergodic regime (due to the scars, etc.), we must perform some averaging over an ensemble of eigenstates, and for this we have chosen 100 consecutive eigenstates. Then, by doing this for all possible data for the the billiard at various λ and k, we ended up with the result that the $R = $ nIPR and A are linearly related and thus also equivalent, as shown in Fig. 1. This is in perfect agreement with the most recent results for the stadium billiard [40], and thus we believe that it is generally true, independent of a specific model system.

In the following we shall use exclusively A as the measure of localization.

D. Introducing the distribution of the localization measure A

The central object of interest in this paper is the distribution $P(A)$ of the localization measures A_m of the chaotic eigenstates within a certain interval of 2000 consecutive even-parity eigenstates indexed by m, around some central value k_0. We have done this for 18 different values of λ and for each λ for 9 to 12 different values of k_0. Each distribution function $P(A)$, generated by the segment of chaotic eigenstates within the stretch of 2000 consecutive values A_m, is defined on a compact interval $[0, A_0]$. Ideally, according to Eqs. (17) and (18), the maximum value of A should be 1, if the Husimi function were entirely and uniformly extended. However, this is never the case, as the Husimi functions have zeros and oscillations, and thus we must expect a smaller maximal value, smaller than 1, which in addition might vary from case to case, depending on k and the grid size. As long as we do not have a theoretical prediction for A_0, we must proceed empirically. Therefore, we have checked several values of A_0 around $A_0 = 0.7$, and found that the latter value is the best according to several criteria. See also the discussion at the end of Sec. IV.

We shall look at the moments of $P(A)$, namely,

$$\langle A \rangle = \int_0^{A_0} A\, P(A)\, dA, \quad \langle A^2 \rangle = \int_0^{A_0} A^2\, P(A)\, dA, \quad (20)$$

and the standard deviation

$$\sigma = \sqrt{\langle A^2 \rangle - \langle A \rangle^2}. \quad (21)$$

For the numerical calculations of the eigenfunctions $\psi_m(\mathbf{r})$ and the corresponding energy levels $E_m = k_m^2$ we have used the Vergini-Saraceno method [55]. Also, we have calculated only the even symmetry class of solutions.

E. The separation of regular and chaotic eigenstates

Now the classification of eigenstates can be performed by their projection onto the classical surface of section. As we are very deep in the semiclassical regime we do expect with probability one that either an eigenstate is regular or chaotic, with exceptions having measure zero, ideally. To automate this task we have ascribed to each point on the grid a number $K_{i,j}$ whose value is either $+1$ if the grid point lies within the classical chaotic region or -1 if it belongs to a classical regular region. Technically, this has been done as follows. We have taken an initial condition in the chaotic region, and iterated it up to about 10^{10} collisions, enough for the convergence (within certain very small distance). Each visited cell (i, j) on the grid has then been assigned value $K_{i,j} = +1$, the remaining ones were assigned the value -1.

The Poincaré-Husimi function $H(q, p)$ Eq. (16) (normalized) was calculated on the grid points and the overlap index M was calculated according to the definition

$$M = \sum_{i,j} H_{i,j}\, K_{i,j}. \quad (22)$$

In practice, M is not exactly $+1$ or -1 but can have a value in between. The reasons are two, first the finite discretization

of the phase space (the finite size grid), and second, the finite wavelength (not sufficiently small effective Planck constant, for which we can take just $1/k_j$). If so, then the question is where to cut the distribution of the M values, at the threshold value M_t, such that all states with $M < M_t$ are declared regular and those with $M > M_t$ chaotic.

There are two natural criteria: (I) *The classical criterion:* the threshold value M_t is chosen such that we have exactly ρ_1 fraction of regular levels and $\rho_2 = 1 - \rho_1$ of chaotic levels. (II) *The quantum criterion:* we choose M_t such that we get the best possible agreement of the chaotic level spacing distribution with the Brody distribution Eq. (6), which is expected to capture the dynamical localization effects of the chaotic eigenstates. However, when we wanted to make sure that only chaotic eigenstates are being used, we have chosen $M_t = 0.5$.

III. MOMENTS OF A AND EXAMPLES OF POINCARÉ-HUSIMI FUNCTIONS

The system parameter governing the localization phenomenon $\alpha = t_H / t_T$, as introduced in Eq. (5), in a quantum billiard described by the Schrödinger equation (Helmholtz equation) Eq. (11), becomes

$$\alpha = \frac{2k}{N_T}, \quad (23)$$

where N_T is the discrete classical transport time, that is the characteristic number of collisions of the billiard particle necessary for the global spreading of the ensemble of uniform in s initial points at zero momentum in the momentum space. This quantity N_T can be defined in various ways as discussed in Refs. [38,39,47,49], where the derivation of t_T, N_T, and α is given. Unlike the stadium billiard, where the diffusion can be very slow and well described by the exponential approach to the equilibrium value (uniformly spread ensemble in the entire phase space), in the present billiard the classical spreading (transport) is not described by a diffusion law but still can be well described by the criterion of the second moment $\langle p^2 \rangle$ reaching a certain fraction (percentage) of the asymptotic, maximal value. Indeed, in spite of some arbitrariness of this definition, we found it sound, as the final results do not qualitatively depend on the choice of the criterion, only some parameters change their values, as we shall see below. In Table I we give the values of N_T according to the four different criteria (50%, 70%, 80%, and 90%), for a variety of values of λ, which we consider in this paper in the sections to follow.

The condition for the occurrence of dynamical localization $\alpha \leqslant 1$ is now expressed in the inequality

$$k \leqslant \frac{N_T}{2}, \quad (24)$$

although the empirically observed transitions are not at all sharp with α.

In Fig. 2 we show the dependence of $\langle A \rangle$ on α, where α is calculated using N_T from Table I. Moreover, to compare and well define the A for various values of λ, we have to divide these values by the relative size (area) χ_C of the largest chaotic component. Otherwise, we would see different values of A even for entirely extended states, due to the different size of the classical chaotic components. Therefore, in the case of

TABLE I. The classical transport time N_T in units of the number of collisions for the criteria of certain percentage of the asymptotic maximal value of the second moment of momentum distribution, starting from zero (Dirac delta distribution), calculated numerically for various values of λ.

	The classical transport time N_T			
λ	90%	80%	70%	50%
0.135	48218	13893	6444	2325
0.140	26830	7992	3750	1227
0.145	21284	5089	2501	936
0.150	11431	3289	1579	534
0.155	6134	2164	1103	405
0.160	3981	1332	706	264
0.165	2506	908	509	205
0.170	1763	678	440	182
0.175	1569	592	327	127
0.180	1257	480	248	86
0.185	737	319	177	62
0.190	542	258	152	55
0.200	314	170	106	47
0.210	287	138	85	37
0.220	192	92	55	23
0.230	147	73	44	17
0.240	106	52	29	9
0.250	77	40	21	7

full extendedness they obtain all the same value A_0, for which it turns out empirically that $A_0 = 0.7$ is the best choice. The table of the χ_C values was published in the paper [47]. Like in the stadium [40,49] the transition from strong localization of small $\langle A \rangle$ and α to the complete delocalization $\alpha \gg 1$ is quite smooth, over almost two decadic orders of magnitude. As we see, $\langle A \rangle$ is approximately fitted by a rational function
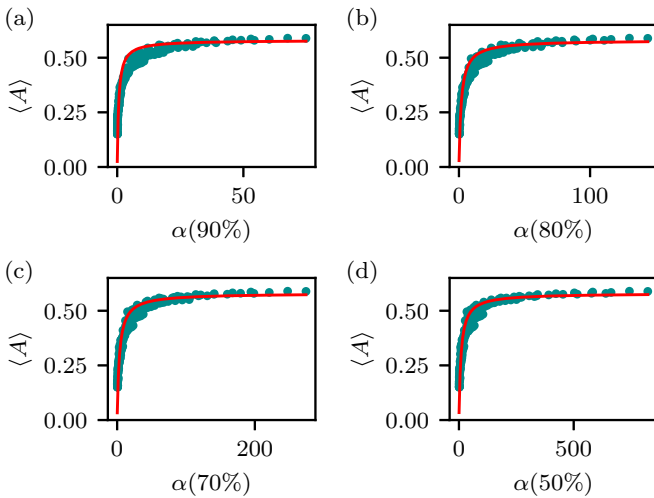

FIG. 2. The mean entropy localization measure $\langle A \rangle$ for variety of λ and energies $E = k^2$, as a function of α fitted by the function Eq. (25), based on N_T from the Table I, with $A_\infty = 0.58$ and $s = 1.70, 0.57, 0.30, 0.11$, for Figs. 2(a)–2(d), respectively. Qualitatively it is very similar to the stadium [40,49].

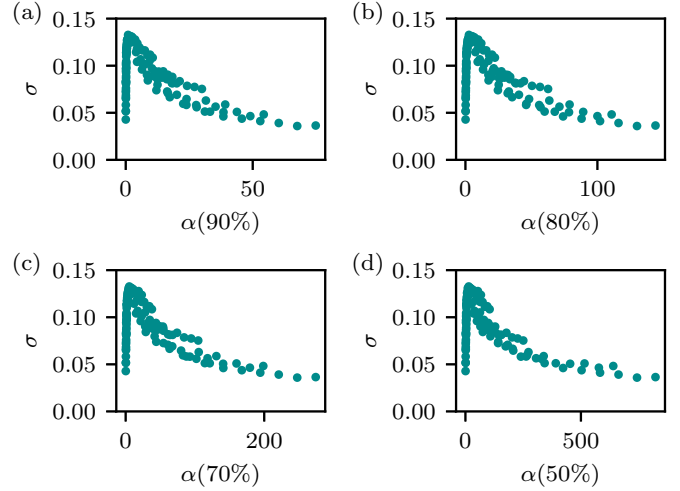
FIG. 3. The standard deviation σ as a function of the α for variety of different shapes λ and energies $E = k^2$. Qualitatively it is very similar to the stadium [40,49].

of α, namely,

$$\langle A \rangle = A_\infty \frac{s\alpha}{1 + s\alpha}, \tag{25}$$

where the values of the parameters are $A_\infty = 0.58$ and $s = 1.70, 0.57, 0.30, 0.11$, for Figs. 2(a)–2(d), respectively.

In Fig. 3 we show the dependence of σ defined in Eq. (21) upon α also using N_T from Table I.

We see that while $\langle A \rangle$ is a monotonically increasing function of α (Fig. 2), the standard deviation σ starts at zero, is small for small α, but rises sharply, and reaches some maximum at about $\alpha \approx 10$, and then decreases very slowly at large values of α. Thus, both the very strongly localized eigenstates, mimicking invariant tori, and the entirely delocalized (ergodic) eigenstates have small spreading σ around the mean value $\langle A \rangle$. According to the quantum ergodic theorem of Shnirelman [9] σ should tend to zero when $\alpha \to \infty$, and rescaled $\langle A \rangle \to 1$, but the transition to that regime might be very slow as suggested by Fig. 3. In this limit $P(A)$ must become the Dirac delta function peaked at A_0. However, it is very difficult to quantify this approach quantitatively, as at large α we have very few physically reliable data points, so it is too early to draw any definite conclusion about the asymptotic behavior at $\alpha \to \infty$. More numerical efforts are needed, currently not feasible.

The Poincaré-Husimi functions describe the structure of the localized chaotic eigenstates. In Fig. 4 we show some selection of typical Poincaré-Husimi functions for various values of λ and k, and the corresponding α. We show only the upper right quadrant $s \in [0, \mathcal{L}/2]$, $p \in [0, 1]$ of the classical phase space, as due to the symmetries (reflection symmetry and the time reversal symmetry) all four quadrants are equivalent. The uniform gray background represents the largest classical chaotic domain, while the darker structures denote the value of the Poincaré-Husimi functions. At large $\lambda = 0.25$ (almost ergodic case) and fixed k, we have small N_T and
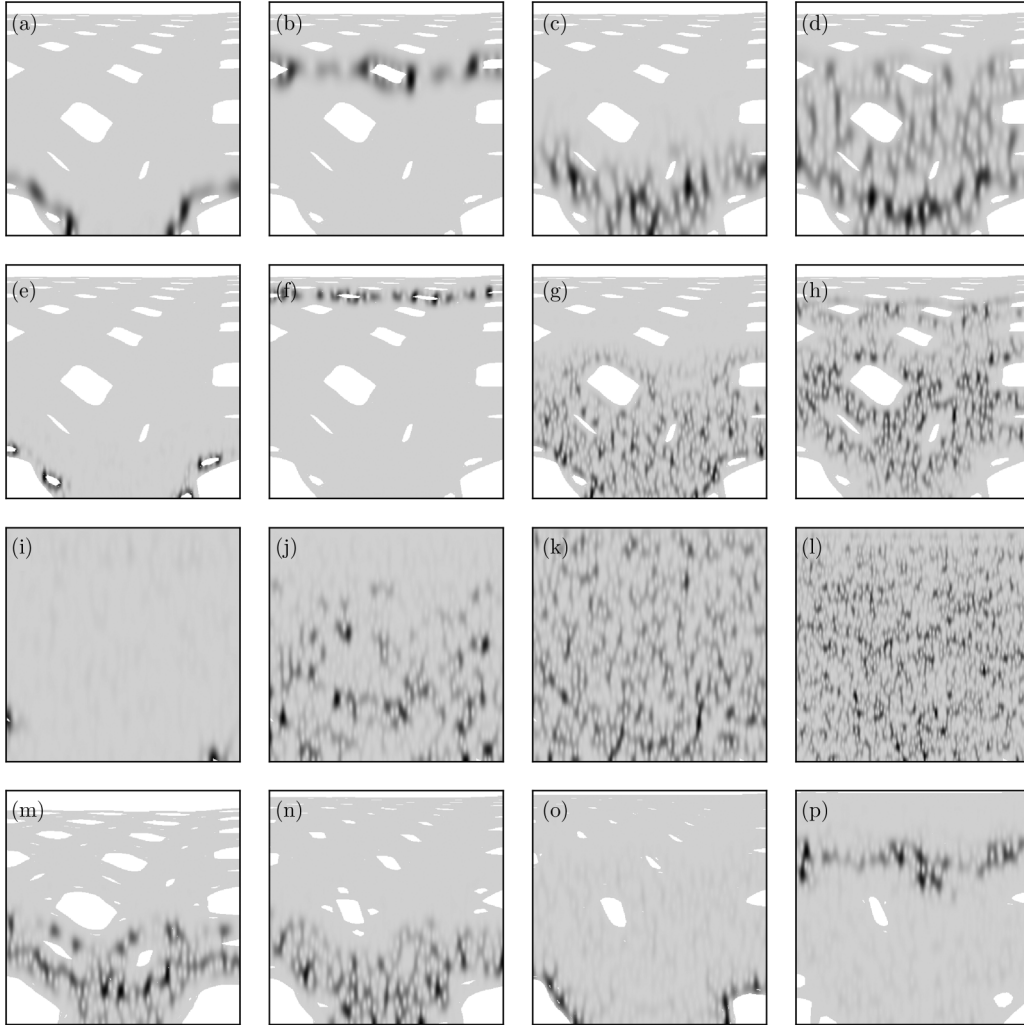
FIG. 4. We show plots of Poincaré-Husimi functions for a representative selection of chaotic eigenstates: Row (a–d): $\lambda = 0.15$, $k = 642.5819901$, 634.10919221, 635.84172768, 634.60937942; Row (e–h): $\lambda = 0.15$, $k = 2598.54009629$, 2598.5812614, 2598.7038606, 2601.4614965; Row (i–l): $\lambda = 0.25$, $k = 640.68503066$, 1197.17988119, 1477.59419041, 3719.0489485; Row (m–p): $\lambda = 0.14$, $k = 1196.82174307$; $\lambda = 0.16$, $k = 1196.83132015$; $\lambda = 0.17$, $k = 1196.87057788$; $\lambda = 0.18$, $k = 1197.13132098$. The uniform gray background represents the largest classical chaotic domain, while the darker structures denote the value of the Poincaré-Husimi functions.

according to Eq. (23) $\alpha \gg 1$, we observe mainly ergodic eigenstates, in agreement with the quantum ergodic theorem [9], that is fully extended states, exemplified in Figs. 4(k) and 4(l). Nevertheless, there are some exceptions, asymptotically of measure zero, where we observe partial localization, as shown in Fig. 4(j). Also, some Poincaré-Husimi functions can be associated with small stability islands around a stable classical orbit exempliifed by Fig. 4(i). Moreover, there can be strongly localized states corresponding to the scaring around and along an unstable periodic orbit in the chaotic sea. More precisely, the area of scars of eigenfunctions $\psi_m(\mathbf{r})$ goes to zero, and the relative number of scarred states goes to zero as $\hbar \to 0$ or $m \to \infty$ [56].

As we decrease $\lambda = 0.15$ and α, thereby increasing N_T, the degree of localization increases, thus $\langle A \rangle$ is decreasing as shown in Figs. 4(a)–4(h). At other values of $\lambda = 0.14, 0.16, 0.17, 0.18$ of strongly pronounced mixed-type phase space we see localized states exemplified in Figs. 4(m)–4(p).

IV. THE DISTRIBUTIONS OF THE LOCALIZATION MEASURES A

In this section we present the central results of this paper, namely, the distribution functions of the localization measures A. It is found, according to our expectation, that in the almost ergodic case with large λ such as, e.g., $\lambda = 0.25$, we find that each distribution can be very well characterized and described by the so-called *beta distribution*,

$$P(A) = CA^a(A_0 - A)^b, \tag{26}$$

where A_0 is the upper limit of the interval $[0, A_0]$ on which $P(A)$ is defined, and the two exponents a and b are positive real numbers, while C is the normalization constant such that $\int_0^{A_0} P(A)\, dA = 1$, i.e.,

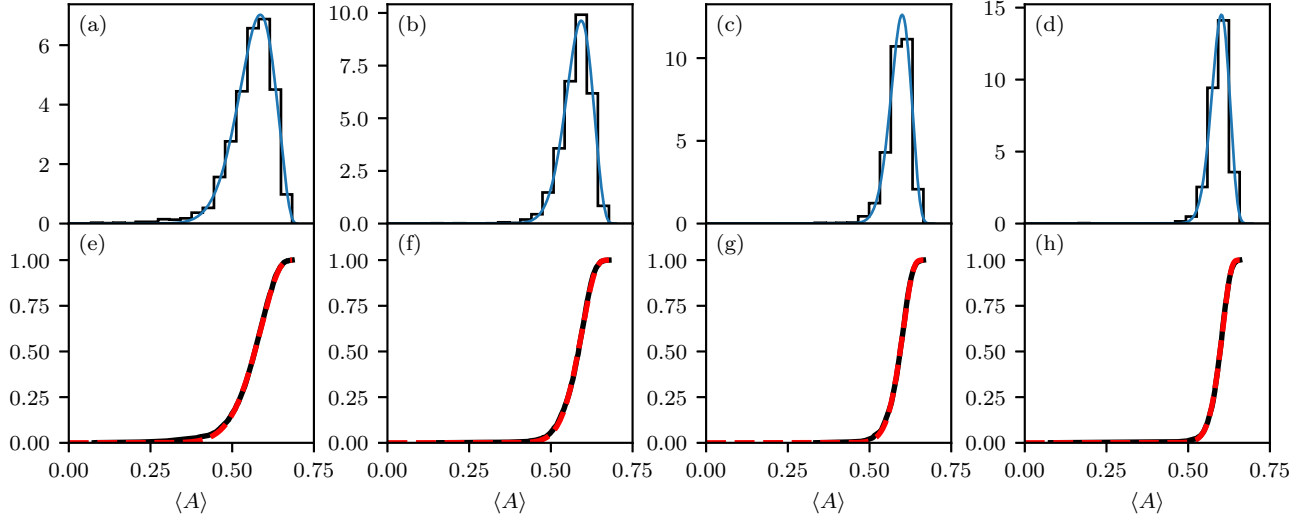$$C^{-1} = A_0^{a+b+1} B(a + 1, b + 1), \tag{27}$$

FIG. 5. The distributions $P(A)$ of the entropy localization measure A for $\lambda = 0.25$ and various k_0 [from (a) to (d), respectively]: 640, 1480, 2600, 3720. (Colors online: black are data, blue is the best fit.) In (e–h) are the corresponding cumulative distributions Eq. (28). (Colors online: black are data, red dashed is the best fit.) It is seen that the beta distribution fit is perfect. $A_0 = 0.7$ and the (a, b) parameters of the best fit beta distribution are from (a) to (d), respectively: (16.57, 3.22), (30.68, 5.55), (50.89, 8.51), (66.61, 10.87).

where $B(x, y) = \int_0^1 t^{x-1}(1-t)^{y-1}dt$ is the beta function. We shall also use the cumulative distribution defined as

$$W(A) = \int_0^A P(x)\, dx. \tag{28}$$

Thus, we have

$$\langle A \rangle = A_0 \frac{a+1}{a+b+3}, \tag{29}$$

and for the second moment

$$\langle A^2 \rangle = A_0^2 \frac{(a+2)(a+1)}{(a+b+4)(a+b+3)}, \tag{30}$$

and therefore for the standard deviation σ Eq. (21),

$$\sigma^2 = A_0^2 \frac{(a+2)(b+2)}{(a+b+4)(a+b+3)^2}, \tag{31}$$

such that asymptotically $\sigma \approx A_0 \frac{\sqrt{b+2}}{a}$ when $a \to \infty$. Whenever we compare A from different λ, we have divided A by the relative fraction of the chaotic component in the classical phase space, denoted by χ_C, as computed and listed in the table of Ref. [47]. In Figs. 5, 6, 7, and 8 we show a selection of typical distributions $P(A)$. In all cases for A_0 we have chosen the empirically best value $A_0 = 0.7$. By k_0 we denote the mean value of k intervals on which we calculate the 2000 successive eigenstates, from which we extract the chaotic ones, by choosing an appropriate value of M_t, always $M_t = 0.5$, to make sure that we collect chaotic states. In addition, it should be noted that losing a few chaotic states, which can happen, does not affect the result for $P(A)$ in any significant way. Also, the statistical significance is very high, which has been carefully checked by using a (factor 2) smaller number of objects in almost all histograms, as well as by changing the size of the boxes.

The limiting case $a \to \infty$ in Eqs. (29) and (31) comprising the fully extended states in the limit $\alpha \to \infty$ shows that the distribution tends to the Dirac delta function peaked at A_0, thus $\sigma = 0$ and $P(A) = \delta(A - A_0)$, in agreement with Shnirelman's theorem [9].

The Fig. 5 clearly shows that the fit by the beta distribution Eq. (26) is excellent in case of $\lambda = 0.25$, typical for the ergodic regimes with $\alpha \gg 1$, as observed also in the stadium in Ref. [40]. The qualitative trend from strong localization to weaker localization or even complete extendedness (ergodicity) with increasing k_0 is clearly visible.

In the Fig. 6 we show the distribution $P(A)$ for $k_0 = 640$ and several values of the shape parameter λ. Here A is normalized by dividing it with χ_C. The behavior that we see is physically very interesting and statistically significant, as we checked carefully, but is not universal, as it depends on the structure of the chaotic component in the classical phase space and on the size and intensity of the stickiness regions. Each stickiness region is expected to support a local maximum in $P(A)$, although this phenomenon is more strongly exhibited in the lemon billiards [57]. Only at large λ, when $\alpha \gg 1$, we see the approach to the beta distribution characteristic of the ergodic regime without stickiness on the underlying chaotic region, exemplified by (j–l), where σ decreases towards the limit $\sigma = 0$. Similar observations apply to Figs. 7 and 8.

We should stress that there is of course some arbitrariness in defining A_0, so long as we do not have a theoretical prediction for its value. So far we have taken $A_0 = 0.7$, but nevertheless tried also the choice of A_0 being the largest member A in each histogram, and found no significant qualitative changes, but only minor quantitative differences. In both cases a and b are *not* unique functions of α, while $\langle A \rangle$ and σ might be unique functions of α as demonstrated in Figs. 2 and 3, and approximated by a fit in Eq. (25).
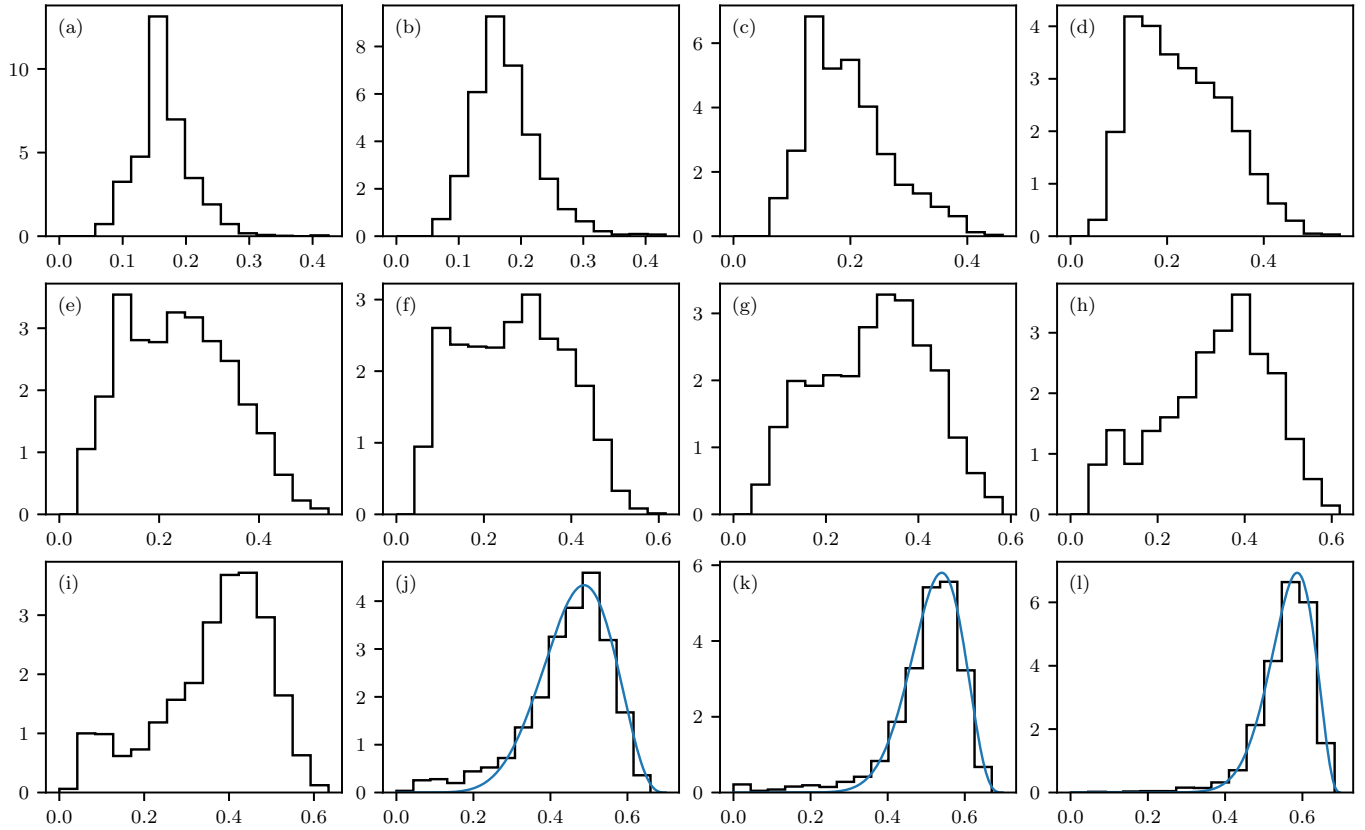
FIG. 6. The distributions $P(A)$ of the entropy localization measure A for $k_0 = 640$ and various λ [from (a) to (l), respectively]: 0.135, 0140, 0.145, 0.150, 0.155, 0.160, 0.165, 0.170, 0.180, 0.200, 0.220, 0.250. The last three histograms (j–l) are well fitted by the beta distribution with $A_0 = 0.7$ and the (a, b) parameter values: (7.56, 3.30), (13.16, 3.89), (16.09, 3.12).

V. IMPLICATIONS OF LOCALIZATION FOR THE SPECTRAL STATISTICS OF CHAOTIC EIGENSTATES

To get a good estimate of β we need many more levels (eigenstates) than in calculating $\langle A \rangle$. The parameter β was computed for 18 different values of the shape parameter λ as given in the Table I, and for 12 intervals in k space: (k_i, k_{i+1}) where $k_i = 500 + 280\,i$ and $i \in [0, 1, \ldots, 11]$. This is $18 \times 12 = 216$ values of β altogether. More than 4×10^6 energy levels were computed for each λ. The size of the intervals in k was chosen to be maximal and such that the BRB (Berry-Robnik-Brody) distribution gives a good fit to the level spacing distributions of the levels in the intervals, meaning that β is well defined.

For each $\beta[\lambda, (k_i, k_{i+1})]$ an associated localization measure $\langle A \rangle$ was computed on a sample of consecutive chaotic levels around $k_0 = \bar{k}_i = (k_i + k_{i+1})/2$, which is a mean value of k on the interval (k_i, k_{i+1}). First, the separation of eigenstates, regular and chaotic, has been done, using $M_t = 0.5$, and then the chaotic eigenstates have been studied. Moreover, the obtained distribution functions $P(A)$ were calculated for 18 values of λ and 9 to 12 values of k_0, and some selection of them is presented and discussed in the previous Sec. IV.

The dependence of β on $\langle A \rangle$, now revised and slightly different than obtained in Ref. [39], where only one value of $\lambda = 0.15$ was used, is shown in Fig. 9. We show two versions of this plot, one with the classical criterion for ρ_1 (for the BRB distribution), and the other one using the quantum criterion for ρ_1, when determining β by fitting the level spacing distribution with the BRB distribution. The two plots are quite similar, which is satisfactory. This relation $\beta(\langle A \rangle)$ is similar to the case of the quantum kicked rotator [33,43,44] and the stadium. In both cases the scattering of points around the mean linear behavior is significant, and it is related to the fact that the localization measure A of eigenstates has some distribution $P(A)$, as observed and discussed in Ref. [58] for the quantum kicked rotator, and discussed for the stadium billiard in the Refs. [40,49].

There is still a great lack in theoretical understanding of the physical origin of this phenomenon, even in the case of (the long standing research on) the quantum kicked rotator, except for the intuitive idea, that energy spectral properties should be only a function of the degree of localization, because the localization gradually decouples the energy eigenstates and levels, switching the linear level repulsion $\beta = 1$ (extendedness) to a power law level repulsion with exponent $\beta < 1$ (localization). The full physical explanation is open for the future.

As shown in Fig. 10, using the classical criterion for ρ_1 for the fitting BRB distribution, the functional dependence of $\beta(\alpha)$ is always the rational function

$$\beta = \beta_\infty \frac{s\alpha}{1 + s\alpha}, \tag{32}$$

only the coefficient s depends on the definition of N_T and α. For the parameter values we get $\beta_\infty = 0.98$ and $s = 1.70, 0.57, 0.30, 0.11$. Similarly, we find for the quantum
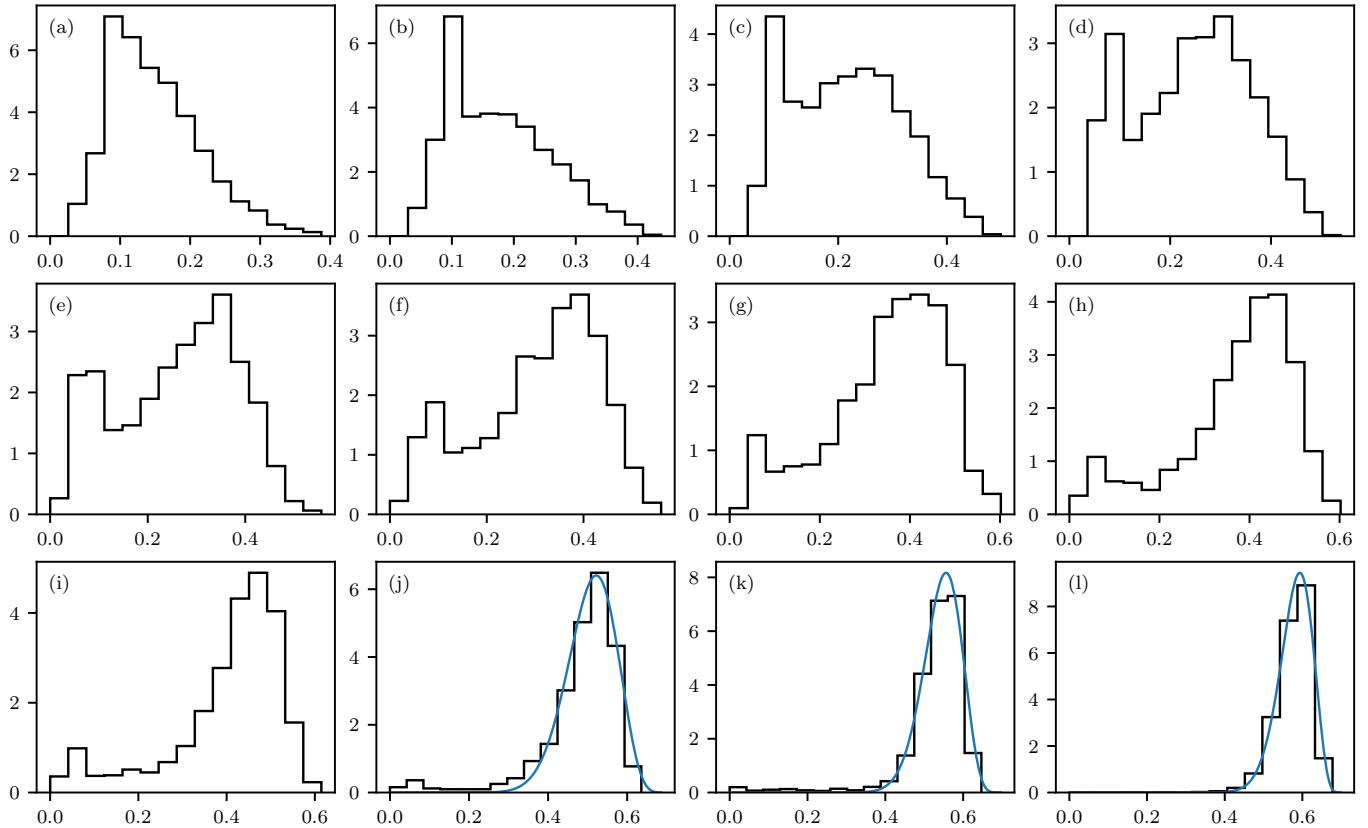
FIG. 7. The distributions $P(A)$ of the entropy localization measure A for $k_0 = 1480$ and various λ [from (a) to (l), respectively]: 0.135, 0140, 0.145, 0.150, 0.155, 0.160, 0.165, 0.170, 0.180, 0.200, 0.220, 0.250. The last three histograms (j–l) are well fitted by the beta distribution with $A_0 = 0.7$ and the (a, b) parameter values: (16.93, 5.79), (25.80, 6.69), (29.36, 5.27).

criterion almost the same results, with no visible differences (not shown).

VI. CONCLUSIONS AND DISCUSSION

In this paper we have studied the structural and statistical properties of the eigenstates and their Poincaré-Husimi functions, and of the energy spectra, of a mixed-type billiard [45,46], in correspondence with its classical dynamics. The governing control parameter is $\alpha = t_H/t_T$, where $t_H = 2\pi\hbar/\Delta E$ is the Heisenberg time and t_T the classical transport time, as in Eq. (5), in the semiclassical regime of sufficiently small effective Planck constant, which is $1/k$ (the wavelength).

To the best of our knowledge our previous [40] and the present work is the first one to study the statistical properties of the localization measures in time-independent Hamilton systems.

Our main conclusions are as follows: (a) We have confirmed that the normalized inverse participation ratio nIPR and the information entropy measure A are linearly related and thus equivalent, in agreement with the recent result in the stadium billiard [40], which we believe is a general result, not specific of the used model systems. (b) We have calculated the Poincaré-Husimi functions of all eigenstates for 18 different values of the shape parameter λ and 9 to 12 values of the starting k_0, in each case 2000 eigenstates of even parity. We have shown a selection of typical Poincaré-Husimi functions.

(c) Then we have separated the regular and chaotic eigenstates, and verified that the chaotic states are localized to the various degree, and calculated the corresponding localization measure A for all of them. (d) We have looked at the distribution functions $P(A)$ and $W(A)$ (histograms and cumulative distributions), and found that in the regime of uniform chaos (no significant stickiness regions in the classical phase space) they are perfectly well described by the beta distribution, which in the limit of $\alpha \gg 1$ approaches the Dirac delta distribution $\delta(A_0 - A)$. This behavior is the same as in the stadium billiard. (e) In the regime of existing pronounced stickiness regions in the classical phase space, $P(A)$ is not universal and can have several maxima (usually it is bimodal), where each minor maximum might be qualitatively attributed to a stickiness region. This phenomenon is under investigation in the lemon billiards [57]. (f) We have explored the mean value $\langle A \rangle$ as a function of α, which is approximately a rational function, while the standard deviation of $P(A)$, denoted by σ, as a function of α, exhibits strong fluctuations but nevertheless displays a similar structure as in the stadium billiard. (g) The level spacing distribution of localized chaotic eigenstates displays the Brody distribution, where the level repulsion exponent β goes from 0 for the strongest localization (Poissonian distribution) to 1 for complete delocalization (ergodicity and GOE). It is a function of $\langle A \rangle$, but slightly different from the result in Ref. [39], where only one value of $\lambda = 0.15$ has been used. It is closer to the linear relationship, which has been observed in the quantum kicked rotator and in the
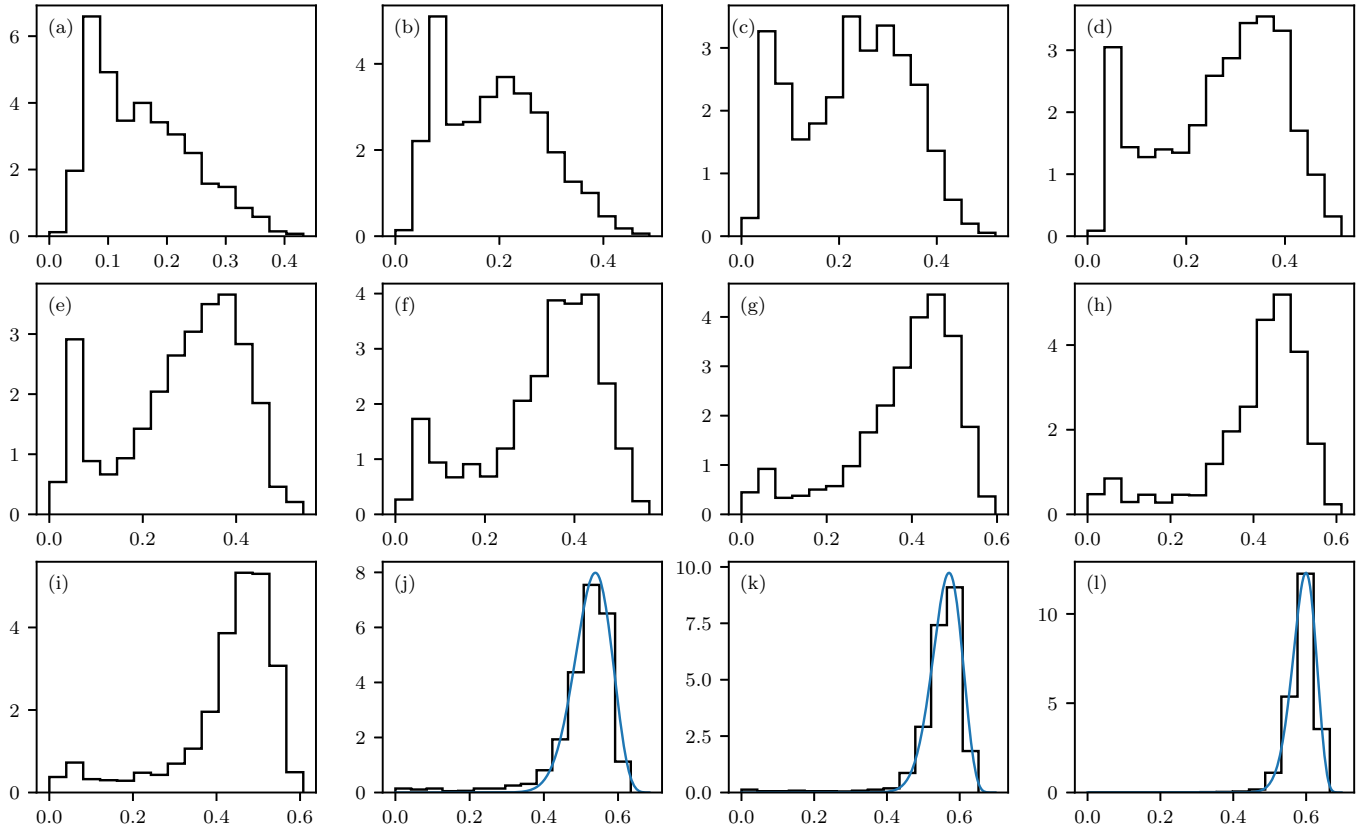
FIG. 8. The distributions $P(A)$ of the entropy localization measure A for $k_0 = 2600$ and various λ [from (a) to (l), respectively]: 0.135, 0140, 0.145, 0.150, 0.155, 0.160, 0.165, 0.170, 0.180, 0.200, 0.220, 0.250. The last three histograms (j–l) are well fitted by the beta distribution with $A_0 = 0.7$ and the (a, b) parameter values: (25.86, 7.74), (35.01, 7.92), (48.46, 8.14).
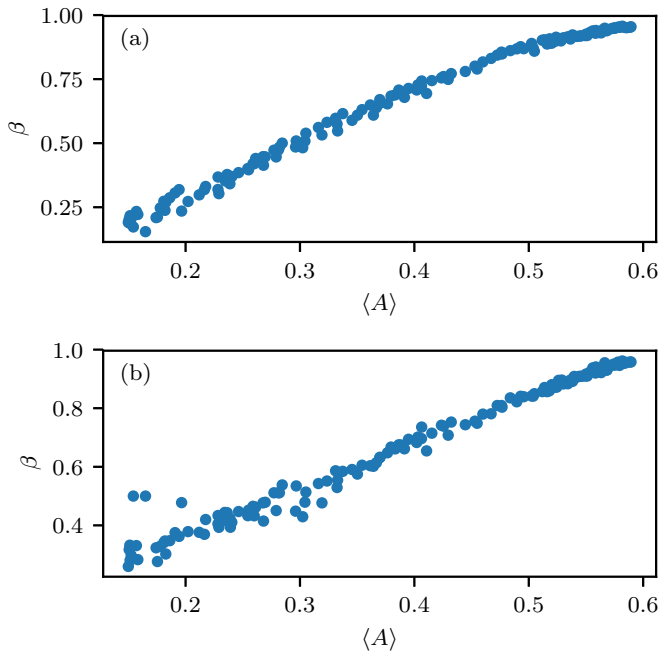

FIG. 9. The level repulsion exponent β as a function of the entropy localization measure $\langle A \rangle$ for variety of λ and energies $E = k^2$, as defined in the text. In (a) we use the classical criterion for ρ_1 and in (b) the quantum one, when calculating β by fitting with BRB ditribution.

stadium billiard, but it also depends slightly on the criterion for choosing ρ_1 in determining β. It must be emphasized that the transition from strong localization $\beta = 0$ to ergodicity $\beta = 1$ as a function of α is a rather smooth one, not a discrete jump, as it takes place over an interval of more than factor 10 in α, which is the same behavior as in the stadium billiard.
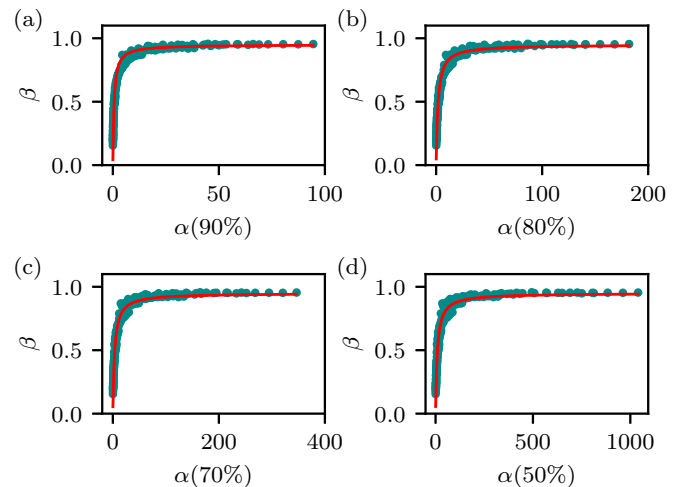

FIG. 10. The level repulsion exponent β, using the classical criterion for ρ_1 for the fitting BRB distribution, as a function of α fitted by the function Eq. (32), based on N_T from the Table I. $\beta_\infty = 0.98$ and $s = 1.70$, 0.57, 0.30, 0.11, for (a–d), respectively.

We believe that our results are new and quite general, typical for the mixed-type Hamiltonian systems, and thus we propose further studies of mixed-type Hamiltonian systems. Where a comparison is applicable, they agree with our quite recent results on the stadium billiard [40,49]. Our similar extensive analysis is being performed also for the lemon billiard [51,57]. The lemon billiard was introduced in Ref. [59] and studied in Refs. [60–63]. Its classical phase space has been very recently extensively explored by Lozej [51]. We expect quite similar results, confirming the general aspects of distribution of localization measures $P(A)$ found in the stadium and the mixed-type billiard.

The major open theoretical question is to derive the existence of dynamical localization in chaotic eigenstates, and to calculate the corresponding $P(A)$, and also the level repulsion exponent β which governs the level spacing distribution, the underlying distribution being close to the Brody distribution. This problem is not yet solved even for the quantum kicked rotator [33]. Further theoretical work is in progress.

We propose the study of localization in the smooth Hamiltonian systems of the mixed-type, such as, e.g., the hydrogen atom in strong magnetic field [64–68] and the Dicke model [69–71], as well as in experiments such as the microwave resonators introduced and performed by Stöckmann since 1990 [1]. We expect similar results as in our three billiard model systems.

ACKNOWLEDGMENT

[1] H.-J. Stöckmann, *Quantum Chaos—An Introduction* (Cambridge University Press, Cambridge, 1999).

[2] F. Haake, *Quantum Signatures of Chaos* (Springer, Berlin, 2001).

[3] M. Robnik, Eur. Phys. J. Special Topics **225**, 959 (2016).

[4] E. Wigner, Phys. Rev. **40**, 749 (1932).

[5] K. Husimi, Proc. Phys. Math. Soc. Jpn. **22**, 264 (1940).

[6] I. C. Percival, J. Phys B: At. Mol. Phys. **6**, L229 (1973).

[7] M. Robnik, Nonl. Phen. in Compl. Syst. (Minsk) **1**, 1 (1998).

[8] M. V. Berry, J. Phys. A: Math. Gen. **10**, 2083 (1977).

[9] B. Shnirelman, Usp. Mat. Nauk **29**, 181 (1974).

[10] A. Voros, Lect. Notes Phys. **93**, 326 (1979).

[11] G. Veble, M. Robnik, and J. Liu, J. Phys. A: Math. Gen. **32**, 6423 (1999).

[12] O. Bohigas, M. J. Giannoni, and C. Schmit, Phys. Rev. Lett. **52**, 1 (1984).

[13] G. Casati, F. Valz-Gris, and I. Guarneri, Lett. Nuovo Cimento **28**, 279 (1980).

[14] M. V. Berry, Proc. Roy. Soc. Lond. A **400**, 229 (1985).

[15] M. Sieber and K. Richter, Phys. Scr. **T90**, 128 (2001).

[16] S. Müller, S. Heusler, P. Braun, F. Haake, and A. Altland, Phys. Rev. Lett. **93**, 014103 (2004).

[17] S. Heusler, S. Müller, P. Braun, and F. Haake, J. Phys. A: Math. Gen. **37**, L31 (2004).

[18] S. Müller, S. Heusler, P. Braun, F. Haake, and A. Altland, Phys. Rev. E **72**, 046207 (2005).

[19] S. Müller, S. Heusler, A. Altland, P. Braun, and F. Haake, New J. Phys. **11**, 103025 (2009).

[20] M. C. Gutzwiller, J. Math. Phys. **8**, 1979 (1967).

[21] M. C. Gutzwiller, J. Math. Phys. **10**, 1004 (1969).

[22] M. C. Gutzwiller, J. Math. Phys. **11**, 1791 (1970).

[23] M. C. Gutzwiller, J. Math. Phys. **12**, 343 (1971).

[24] M. C. Gutzwiller, Phys. Rev. Lett. **45**, 150 (1980).

[25] M. V. Berry and M. Robnik, J. Phys. A: Math. Gen. **17**, 2413 (1984).

[26] T. Prosen and M. Robnik, J. Phys. A: Math. Gen. **32**, 1863 (1999).

[27] B. V. Chirikov, F. M. Izrailev, and D. L. Shepelyansky, Sov. Sci. Rev. C **2**, 209 (1981).

[28] G. Casati, B. V. Chirikov, F. M. Izrailev, and J. Ford, Lecture Notes Phys. **93**, 334 (1979).

[29] F. M. Izrailev, Phys. Rev. Lett. **56**, 541 (1986).

[30] F. M. Izrailev, Phys. Lett. A **125**, 250 (1987).

[31] F. M. Izrailev, Phys. Lett. A **134**, 13 (1988).

[32] F. M. Izrailev, J. Phys. A: Math. Gen. **22**, 865 (1989).

[33] F. M. Izrailev, Phys. Rep. **196**, 299 (1990).

[34] F. Borgonovi, G. Casati, and B. Li, Phys. Rev. Lett. **77**, 4744 (1996).

[35] L. Bunimovich, Commun. Math. Phys. **65**, 295 (1979).

[36] T. Prosen, in *Proceedings of the International School of Physics*, edited by G. Casati and U. Smilansky (IOS Press, Amsterdam, 2000).

[37] B. Batistić and M. Robnik, J. Phys. A: Math. Theor. **43**, 215101 (2010).

[38] B. Batistić and M. Robnik, Phys. Rev. E **88**, 052913 (2013).

[39] B. Batistić and M. Robnik, J. Phys. A: Math. Theor. **46**, 315102 (2013).

[40] B. Batistić, Č. Lozej, and M. Robnik, J. Phys. A: Math. Theor. (to be published) (2019).

[41] T. A. Brody, Lett. Nuovo Cimento **7**, 482 (1973).

[42] T. A. Brody, J. Flores, J. B. French, P. A. Mello, A. Pandey, and S. S. M. Wong, Rev. Mod. Phys. **53**, 385 (1981).

[43] T. Manos and M. Robnik, Phys. Rev. E **87**, 062905 (2013).

[44] B. Batistić, T. Manos, and M. Robnik, EPL **102**, 50008 (2013).

[45] M. Robnik, J. Phys. A: Math. Gen. **16**, 3971 (1983).

[46] M. Robnik, J. Phys. A: Math. Gen. **17**, 1049 (1984).

[47] Č. Lozej and M. Robnik, Phys. Rev. E **98**, 022220 (2018).

[48] Č. Lozej and M. Robnik, Phys. Rev. E **97**, 012206 (2018).

[49] B. Batistić, Č. Lozej, and M. Robnik, Nonlin. Phenom. Complex Syst. (Minsk) **21**, 225 (2018).

[50] R. Markarian, Nonlinearity **6**, 819 (1993).

[51] Č. Lozej (unpublished).

[52] M. V. Berry, Eur. J. Phys. **2**, 91 (1981).

[53] J. Tualle and A. Voros, Chaos Solitons Fract. **5**, 1085 (1995).

[54] A. Bäcker, S. Fürstberger, and R. Schubert, Phys. Rev. E **70**, 036204 (2004).

[55] E. Vergini and M. Saraceno, Phys. Rev. E **52**, 2204 (1995).

[56] E. J. Heller, Phys. Rev. Lett. **53**, 1515 (1984).

[57] Č. Lozej, D. Lukman, and M. Robnik (unpublished).

[58] T. Manos and M. Robnik, Phys. Rev. E **91**, 042904 (2015).

[59] E. J. Heller and S. Tomsovic, Phys. Today **46**(7), 38 (1993).

[60] V. Lopac, I. Mrkonjic, and D. Radic, Phys. Rev. E **59**, 303 (1999).

[61] V. Lopac, I. Mrkonjic, and D. Radic, Phys. Rev. E **64**, 016214 (2001).

[62] H. Makino, T. Harayama, and Y. Aizawa, Phys. Rev. E **63**, 056203 (2001).

[63] L. A. Bunimovich, G. Casati, T. Prosen, and G. Vidmar, Exp. Math. **1**, 10 (2019).

[64] M. Robnik, J. Phys. A: Math. Gen. **14**, 3195 (1981).

[65] M. Robnik, J. Phys. Colloques **43**, C2-45 (1982).

[66] H. Hasegawa, M. Robnik, and G. Wunner, Prog. Theor. Phys. Suppl. (Kyoto) **98**, 198 (1989).

[67] H. Friedrich and H. Wintgen, Phys. Rep. **183**, 37 (1989).

[68] H. Ruder, G. Wunner, H. Herold, and F. Geyer, *Atoms in Strong Magnetic Fields* (Springer, Heidelberg, 1994).

[69] R. H. Dicke, Phys. Rev. **93**, 99 (1954).

[70] K. Furuya, M. C. Nemes, and G. Q. Pellegrino, Phys. Rev. Lett. **80**, 5524 (1998).

[71] M. A. Bastarrachea-Magnani, B. L. del Carpio, S. Lerma-Hernandez, and J. G. Hirsch, Phys. Scr. **90**, 068015 (2015).